catalysts

MDPI

Article

Magnetic Metallic Nanoparticles Coated with Carbon for the Catalytic Removal of Bromate from Water

Patrícia S. F. Ramalho [1,2], Olívia Salomé G. P. Soares [1,2,*], José J. M. Órfão [1,2] and Manuel Fernando R. Pereira [1,2]

[1] LSRE-LCM—Laboratory of Separation and Reaction Engineering—Laboratory of Catalysis and Materials, Faculty of Engineering, University of Porto, Rua Dr. Roberto Frias, 4200-465 Porto, Portugal; up200605969@edu.fe.up.pt (P.S.F.R.); jjmo@fe.up.pt (J.J.M.Ó.)

[2] ALiCE—Associate Laboratory in Chemical Engineering, Faculty of Engineering, University of Porto, Rua Dr. Roberto Frias, 4200-465 Porto, Portugal

* Correspondence: salome.soares@fe.up.pt

Abstract: Bromate, often detected in drinking water, is associated with a significant risk of cancer. Catalytic reduction has been recognized as an effective treatment technique to remove ions by reducing them over metal catalysts in the presence of a reducing agent, usually hydrogen. This work aims to synthesize metallic magnetic nanoparticles of iron oxide (FeO) and mixed iron oxides with manganese (MnFeO), cobalt (CoFeO), and copper (CuFeO) coated with carbon via chemical vapor deposition (C-MNP) to be applied as catalysts to the reduction of bromate in water. The use of magnetic nanoparticles coated with carbon enables catalyst recovery via magnetic separation and takes advantage of the catalytic properties of the carbon materials. The iron particles proved to be the most promising catalysts for the reduction of bromate into bromide, the highest removal being obtained with the CFeO@CVD750 sample, resulting in a 99% conversion after 120 min of reaction under the conditions tested. Due to its magnetic nature, the catalytic material was easily removed after the reaction and applied in four consecutive cycles without losing its catalytic properties. These results highlight the great potential of carbon-coated magnetic nanoparticles for reducing bromate in water.

Keywords: metallic magnetic materials; chemical vapor deposition; bromate reduction; carbon

Citation: Ramalho, P.S.F.; Soares, O.S.G.P.; Órfão, J.J.M.; Pereira, M.F.R. Magnetic Metallic Nanoparticles Coated with Carbon for the Catalytic Removal of Bromate from Water. *Catalysts* **2024**, *14*, 149. https://doi.org/10.3390/catal14020149

Academic Editor: Jean-François Lamonier

Received: 31 December 2023
Revised: 7 February 2024
Accepted: 14 February 2024
Published: 17 February 2024

1. Introduction

Drinking water is often contaminated with oxyanions such as nitrate (NO_3^{--}), bromate (BrO_3^-), perchlorate (ClO_4^-), and arsenic (AsO_3^{3-} or AsO_4^{3-}), which can pose major health risks [1].

Bromate is normally produced in treatment processes involving the ozonation or chlorination of water containing bromide [2,3]. To minimize bromate formation, water treatment plants must carefully control disinfection processes, adjusting reaction conditions and optimizing ozone dosage [4]. Several studies have confirmed that bromate is a carcinogen, posing a threat to humans [3,5]. As such, the International Agency for Cancer Research (IARC) has classified bromate as a group 2B substance [5,6]. Therefore, the World Health Organization (WHO) and the United States Environmental Protection Agency (EPA) have recommended a maximum contaminant level of 0.078 μmol L^{-1} (10 μg BrO_3^- L^{-1}) for bromate in drinking water [5,7]. The bromide ion has a low degree of toxicity, and bromine is not listed as a carcinogen by the International Agency for Research on Cancer (IARC) [8]. As such, this ion does not represent a concern for human health.

Several methods, such as ion exchange [9,10], photocatalysis [11,12], adsorption [13,14], electrochemical reduction [15,16], UV irradiation [17,18], and heterogeneous catalytic reduction under hydrogen [7,19], have been developed to remove bromate from drinking water. Catalytic reduction is considered a promising technology for this type of treatment because

it generally uses readily available hydrogen as a reducing agent and can eliminate various contaminants from water without forming toxic by-products [5,7,20]. Among several noble metals, Pd has been widely considered the most effective catalyst for reducing bromate into bromide [20,21]. Chen et al. [20] studied the use of Pd and Pt supported on alumina, finding that both types presented significant and promising results. However, Pd-based catalysts stood out as the most active, possibly due to their greater capacity for dissociative H_2 adsorption. The efficiency of commercial catalysts containing activated carbon or alumina with different metals, such as Pd, Pt, Ru, Rh, and Ir [22], was compared, revealing distinct catalytic performances influenced by the selected metal, metal content, and pH. At a neutral pH, catalysts with Rh and Ir showed greater activity, while, when reducing the pH to 3.0, catalysts based on Pd and Pt demonstrated the best results. However, the Ru catalyst exhibited the lowest activity under both pH conditions. On the other hand, the study of Restivo et al. [3] on activated carbon-based catalysts supporting 1 wt% of various metals (Pt, Pd, Cu, Sn, Rh, Ru, Ni, Ir, Fe, or Zn) revealed a 90% conversion using non-noble metals after 120 min, while noble metals achieved almost complete conversion. Although the Pt catalysts demonstrated the highest activity, the Pd catalyst proved to be more efficient in bromate conversion. The catalytic results were associated with the dissociative chemisorption energy of hydrogen on the different metals, showing that the most active catalysts were those with a medium-strength bond with hydrogen. Additionally, the application of bimetallic catalysts for the catalytic hydrogenation, combining a noble and a non-noble metal, of other inorganic pollutants in water, such as nitrate [23,24], was investigated. The results suggest that the presence of a second metal impairs the hydrogenative activity of the noble metal [5,23]. However, Pd–Cu bimetallic catalysts showed a slight improvement in catalytic activity, although this improvement was not considered sufficient to justify the combined use of both metals.

On the other hand, in recent years, there has been a great interest in the study of supermagnetic nanoparticles due to their high surface area, supermagnetism, sorption capability, and catalytic properties [25,26]; they have gained increasing importance in several areas such as biomedicine/biotechnology [27–29], catalysis [30–33], and water treatment [26,34–38]. Magnetic nanoparticles (MNPs) can be coated with a layer of different materials to improve their stability and introduce new properties and functionalities on the surface. Carbon materials are widely used as catalyst supports, but their use as catalysts has attracted a lot of attention [7]. The combination of carbon materials with magnetic nanoparticles offers the possibility of creating composite materials with synergistic properties, taking into consideration the catalytic properties of both substances and the magnetic nature of magnetic nanoparticles [26]. The use of magnetic catalysts may show advantages in liquid systems. For example, the solid magnetic catalyst may be separated via an external magnet after the reaction and then reused in the next batch, thereby preventing catalyst loss and increasing its durability [39]. In the case of bromate reduction, only a few studies are reporting the application of magnetic nanoparticles in the catalytic reduction process [38,40,41]. Li et al. [38] studied the catalytic reduction of bromate over Pd nanoparticles supported on shell- and core-structured magnetites with different shells (e.g., carbon, SiO_2, polypyrrole, polyaniline, polydopamine, and chitosan), revealing that the catalyst that had a greater catalytic activity was the Pd supported on the Fe_3O_4 composite coated with polyaniline (Pd/Fe_3O_4@PANI); it was found that 0.4 mM of bromate can be completely reduced into bromide after 120 min under the selected conditions.

The heterogeneous catalytic reduction of bromate into bromide usually uses noble metal catalysts, such as Pd, Pt, Ru, and Rh, as they exhibit high catalytic activities. However, these catalysts are quite expensive, and conventional separation methods such as centrifugation and filtration are complicated, time-consuming, and subject to material loss. In the present study, magnetic nanoparticles, composed of iron oxides coated with carbon through chemical vapor decomposition (CVD), will be developed and evaluated in the

bromate reduction in water, as it is a cheaper material, and its magnetic properties provide a viable separation process to recover the catalyst.

2. Results

2.1. Materials Characterization

N_2 adsorption–desorption isotherms were performed at −196 °C to evaluate the textural properties of the materials prepared.

Table 1 shows the textural characterization of all samples under study, revealing that the magnetic particles have a specific surface area between 101 and 235 $m^2\ g^{-1}$. The introduction of cobalt (Co) and copper (Cu) in the preparation of the FeO particles increases the surface area compared to the particles prepared only with iron (154 $m^2\ g^{-1}$). On the other hand, the surface area decreases (101 $m^2\ g^{-1}$) when manganese (Mn) is introduced.

Table 1. The textural properties and carbon and metal content of the MNP materials.

Sample	S_{BET} ($m^2\ g^{-1}$)	% Carbon	% Metal
FeO	154	-	98
CFeO@CVD750	63·	16	84
2%Fe_CNT	266	98	2
MnFeO	101	-	98
CMnFeO@CVD750	45·	22	78
CoFeO	184	-	96
CCoFeO@CVD750	29·	34	66
CuFeO	235	-	96
CCuFeO@CVD750	27·	33	67

· S_{BET} of these materials was calculated per gram of carbon (determined via TGA).

For the magnetic particles coated with carbon, the surface area was calculated per gram of carbon determined by thermogravimetric analysis (TGA). For this type of sample, it was observed that the specific surface area (calculated per gram of carbon) decreases drastically to values lower than 10 $m^2\ g^{-1}$ [26].

The sample prepared via the incipient impregnation method (2%Fe_CNT) has the highest specific surface area. CNTs are mesoporous materials with a surface area of 283 $m^2\ g^{-1}$ [26], and when introducing iron, the specific surface area decreases slightly (266 $m^2\ g^{-1}$) due to the small amount of metal (2 wt.%).

The TPR profiles of CuFeO, FeO, CCuFeO@CVD750, and CFeO@CVD750 are shown in Figure 1. The CuFeO sample (Figure 1a) shows two reduction peaks similar to those observed in the FeO profile (Figure 1b). The first peak occurred between 200 and 400 °C, at which point the reduction of $CuFe_2O_4$ to Cu^0 and Fe_3O_4 occurs. The peak at higher temperatures is related to the reduction of Fe_3O_4 to Fe [26,42,43]. In Figure 1b, it is possible to observe the characteristic reduction peaks of Fe_2O_3 nanoparticles. The first peak (between 300 and 400 °C) corresponds to the reduction of Fe_2O_3 to Fe_3O_4. Then, between 400 and 700 °C, the second peak is assigned to the sequential reduction from Fe_3O_4 to FeO and, finally, Fe^0 [26,43]. After coating with carbon through the CVD process, these peaks were not observed due to the encapsulation of the oxides via carbon material. Cobalt reduction generally exhibits two peaks between 300 and 500 °C, associated with two Co_3O_4 reduction steps ($Co_3O_4 \rightarrow CoO \rightarrow Co^0$) [26,43]. The TPR profile of CoFeO (Supplementary Figure S1a) reveals a significant reduction peak reaching a maximum near 600 °C, related to the formation of magnetite (Fe_3O_4), together with the reduction of Co_3O_4 to Co^0 [26,43,44]. In the same way, as observed with other MNP materials, no further metal reduction peaks were detected after carbon coating via CVD. In the case of MnFeO (Supplementary Figure S1b), the reduction process can be explained as $MnFe_2O_4 \rightarrow MnFe_2O_4-\delta \rightarrow$ MnO-FeO $\rightarrow$ α-FeO. Therefore, the reduction peak around 350 °C tends to be lower, while the peak between 400 and 600 °C is more pronounced. After 600 °C, the third peak indicates the degradation of the $MnFe_2O_4$ structure, indicating the formation of Fe_2O_3. Therefore, in

addition to providing $MnFe_2O_4$ ferrite, this type of material also reveals the presence of Fe_2O_3 in its structure [26,43,45]. After carbon coating via CVD, these peaks were no longer identified, which can be explained for the same reasons presented previously.

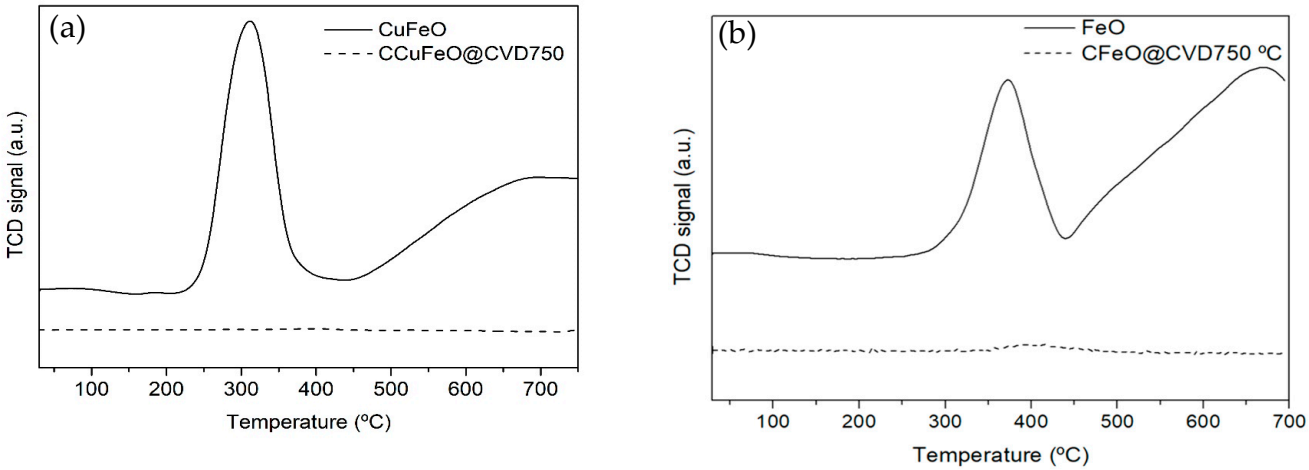

Figure 1. TPR profiles of samples: (**a**) CuFeO and CCuFeO@CVD750 and (**b**) FeO and CFeO@CVD750.

The TPR profile of the 2%Fe_CNT shows that the major reduction peak occurs at 380 °C [26].

SEM images of the magnetic particles are shown in Figure 2. This characterization technique was used to obtain three-dimensional images of the external morphology of the materials, as well as their composition.

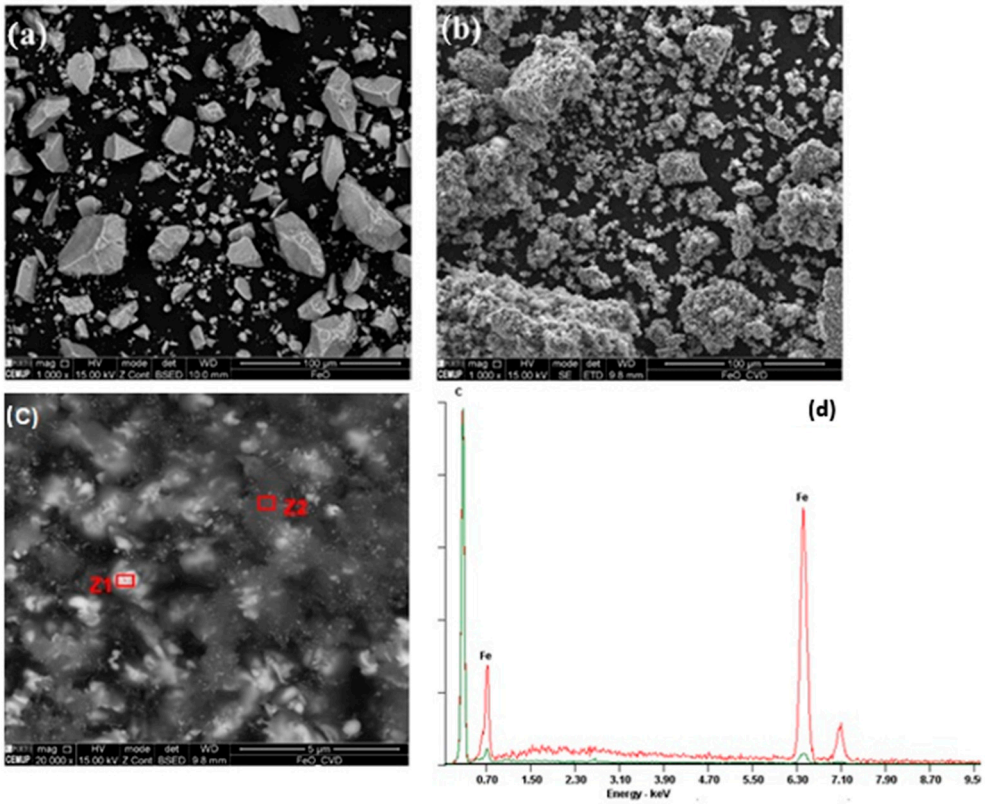

Figure 2. SEM–EDS images of selected samples: (**a**) FeO and (**b**–**d**) CFeO@CVD750 (Z1: red; Z2: green spectra and red squares are analysis zones).

Figure 2a shows that the FeO particles are very small. When analyzing Figure 2b,c, it is observed that carbon-coated FeO particles become larger and heterogeneous. In the SEM image with energy-dispersive X-ray spectroscopy, the lighter areas (zone Z1) refer to the metal due to its higher atomic number. On the other hand, the darkest areas (zone Z2) predominantly contain carbon, as demonstrated in the spectra of Figure 2d.

Figure 3 shows the TEM micrographs of the FeO and CFeO@CVD750 catalysts, and it is possible to observe the presence of carbon in the sample prepared via CVD. For the FeO sample, the metallic particles have a reduced spherical shape not well defined, with sizes between approximately 1 and 30 nm. In contrast, after being subjected to the CVD process, the particles are well defined and have a significantly larger size, and it is possible to observe the metal encapsulated inside the particles, which could be the reason for the drastic reduction in surface area (Table 1).

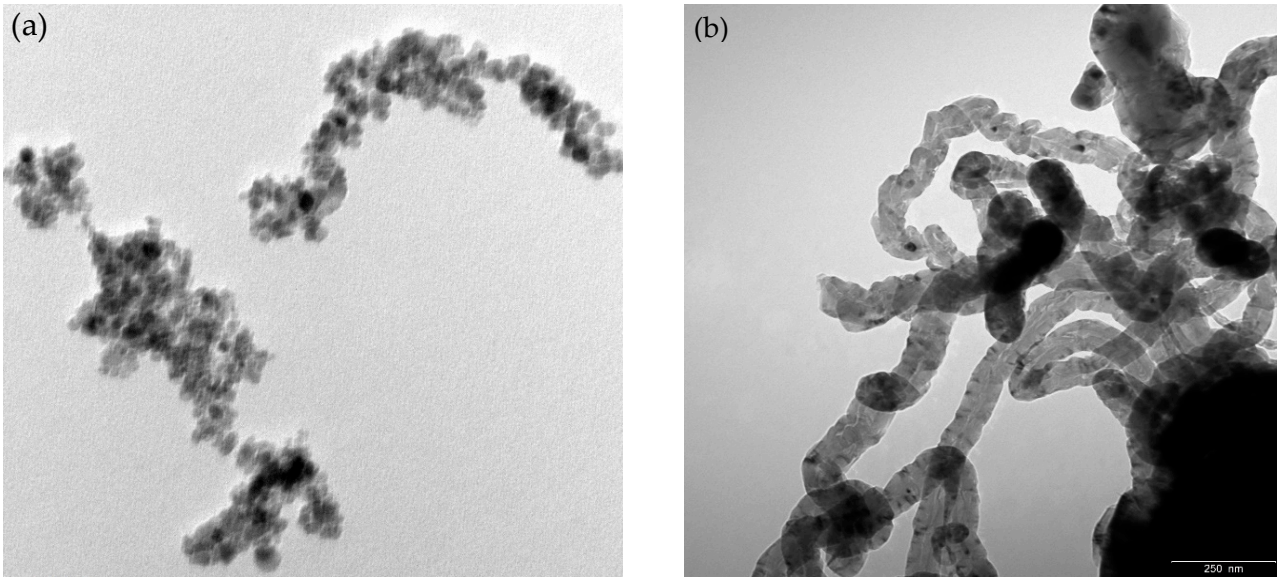

Figure 3. TEM micrographs of selected samples: (**a**) FeO and (**b**) CFeO@CVD750.

The FeO and CFeO@CVD750 catalysts were analyzed via X-ray diffraction (XRD) (Figure S2, Supplementary Materials), showing that the magnetic iron particles have the characteristic peaks of iron oxides. This type of nanoparticle has a typic diffractogram pattern of ferrite, confirming the expected structure of cubic spinel (Fd3m) [25,26]. Table 2 shows the phases identified and the crystallite sizes for the magnetic particles of iron before and after carbon coating.

Table 2. Properties of selected materials obtained through XRD analysis.

Sample	Phase (%V/V)	Crystallite Size (nm)
FeO	Magnetite = 100	20.5 ± 0.5
	Cementite (Fe_3C) = 3.0	84 ± 10
CFeO@CVD750	Fe α = 1.6	72 ± 5
	Grafite = 95.4	16 ± 1

The XRD analyses of the magnetic nanoparticles show that the FeO sample presents only a single phase (magnetite), while the corresponding sample with carbon prepared through CVD has a large amount of carbon in its composition, thus appearing as graphite with a percentage of 95%, as expected. Through XPS analysis of the binding energies of the Fe 2p3/2 peak, it was found that the FeO sample contains a significant amount of iron in its composition, representing 54.5% of the total weight [26]. In this sample, iron is present in the Fe^{2+} and Fe^{3+} forms. In contrast, in the CFeO@CVD750 sample, only 0.37% of the

iron was identified in the Fe^{2+} and Fe^{3+} forms since its surface is predominantly composed of carbon, representing 96.7% of the total weight. These proportions agree with the results obtained via TPR, indicating that the metal is encapsulated by carbon.

2.2. Catalytic Tests

2.2.1. Bromate Reduction over Magnetic Nanoparticles

The kinetic results for the bromate reduction under hydrogen flow using magnetic nanoparticles as catalysts are shown in Figure 4a, and the dimensionless concentrations of bromate and bromide after 120 min of reaction are shown in Figure 4b. A non-catalytic test was also carried out as a control experiment, which presented a 40% bromate removal after 120 min of reaction. This result is in accordance with the literature [3,7], which reported that bromate reacts with hydrogen in solution, being one of the ways to reduce bromate. A study of bromate catalytic reduction under hydrogen, using metal catalysts supported on activated carbon, identified four possible ways in which the reaction could occur: (1) direct reaction with hydrogen in solution, without interaction with the catalyst; (2) bromate adsorption and its reduction via hydrogen on the surface of the activated carbon; (3) adsorption of bromate on the surface of the activated carbon; and (4) adsorption and reduction on the surface of metallic particles of the catalyst. Although bromate is reduced in different ways, the most important mechanism corresponds to the dissociative adsorption of hydrogen on the metal surface and the reaction of adsorbed hydrogen with bromate [3,7].

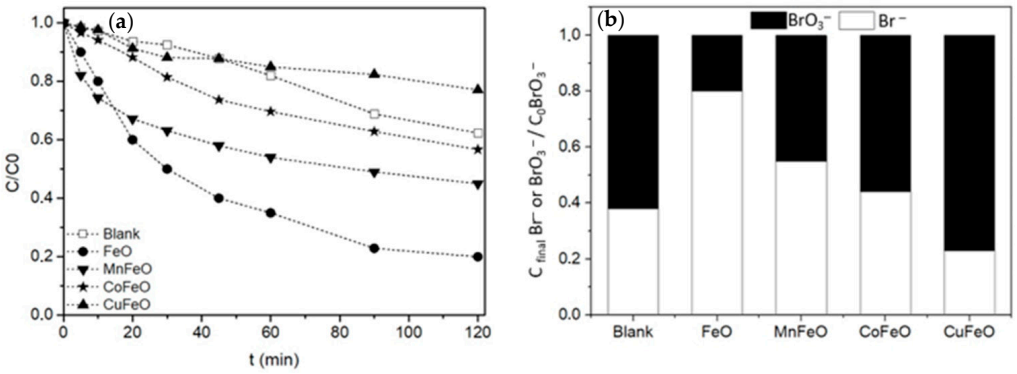

Figure 4. Bromate reduction with hydrogen in the presence of magnetic nanoparticles as a function of (**a**) time and (**b**) bromate and bromide dimensionless concentrations after 120 min of reaction.

The catalyst's efficiency is inherently connected to various elements, including the distribution of metals, the characteristics of these metals, the support material employed, and the engagement with H_2 in water. The significance of this final factor is pivotal for the overall functionality of the catalyst. An investigation focused on determining the quantity of H_2 needed to activate the catalyst by varying H_2 flow rates from 5 to 75 cm^3 min^{-1} revealed a generally consistent activation pattern, except for a flow rate of 5 cm^3 min^{-1} [4]. Therefore, the determination of the H_2 flow rate is an important step since, as mentioned earlier and as suggested in the literature, the reaction mechanism involves the dissociative adsorption of H_2 on the surface of the metallic catalyst and the reaction between the adsorbed bromate ions and the atoms of hydrogen [3].

Figure 4a reveals that the highest bromate removal was achieved in the presence of FeO. When other metals (Mn, Co, and Cu) were incorporated into the iron catalyst, the conversion after 120 min decreased from 80% to 55, 44, and 23%, respectively, presenting a removal similar to the non-catalytic run and indicating that these metals do not present any catalytic activity for bromate reduction. Soares et al. [7] studied the reduction of bromate in H_2 on Pd, Cu, and PdCu catalysts supported on carbon nanotubes and found that copper catalysts do not improve bromate removal, presenting a performance similar to the test

without a catalyst. It can be concluded that the CuFeO catalyst is not a suitable catalyst for the removal of bromate.

The better performance of the FeO catalyst during the reduction of bromate to bromide may be related to the chemisorption of H_2 on metals and through oxidation/reduction states. According to Hagen [46], transition metals have a higher chemisorption capacity, followed by metals belonging to groups 4–8 of the periodic table, which is the case of cobalt. On the other hand, manganese and copper, two metals of the first period of transition metals, exhibit "abnormal" behavior and display weak H_2 chemisorption, which explains the better catalytic activity of the FeO catalyst. It is also worth noting that the samples underperformed the FeO sample, suggesting that FeO is the active phase and that it is not worth introducing a new metal to the FeO.

Shen et al. [6] investigated bromate removal with core–shell $Fe@Fe_2O_3$ nanowires and found that these showed good performance in bromate removal. Fe (II) is adsorbed on the iron oxide surface and forms $Fe(II)_{bound}$, accelerating bromate reduction due to its greater reducing capacity. Xie et al. [47] studied the effect of Fe (III) on the reduction of bromate via humic substances in an aqueous solution, in which Fe (III) was reduced to Fe (II) and, thus, increased the rate of bromate reduction via humic substances. Zhong et al. [48] reported that Fe (II) in Fe-Al LDH (type SO4) first adsorbs bromate and then reduces it to bromide and transfers Fe^{2+} to FeOOH.

2.2.2. Bromate Reduction over Magnetic Nanoparticles Coated with Carbon

The catalytic activity of the magnetic samples was further evaluated for the bromate reduction by coating them with carbon via chemical vapor decomposition (CVD) at 750 °C. For comparative purposes, a monometallic catalyst of iron supported on CNTs (2% Fe_CNT) was also prepared. Figure 5 shows that all the carbon-based magnetic nanoparticles perform better than uncoated magnetic nanoparticles (cf. Figure 4), revealing that carbon plays an important role during the catalytic reduction process.

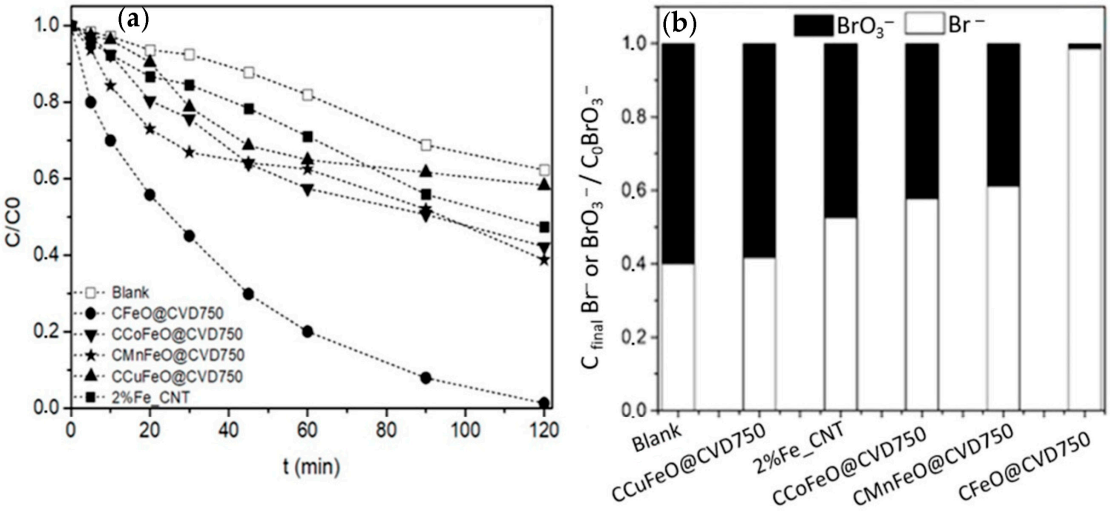

Figure 5. Bromate reduction with hydrogen in the presence of magnetic nanoparticles coated with carbon as a function of (**a**) time and (**b**) bromate and bromide dimensionless concentrations after 120 min of reaction; the results obtained with the Fe monometallic catalyst supported on CNTs (2%Fe_CNT) are also included for comparison.

Carbon materials have good chemical stability and the ability to customize their textural and surface chemical properties. As such, the best results were obtained with the incorporation of carbon in the magnetic nanoparticles. As can be seen through the analysis of the TEM micrographs, the magnetic nanoparticles were encapsulated in carbon after the treatment using CVD, resulting in the carbon phase being the main phase responsible for improving the activity.

The introduction of Co, Mn, or Cu into the FeO particles, followed by the coating of the particles with carbon via CVD, does not improve the catalytic performance, bromate removals of 61%, 58%, and 42%, respectively, being obtained, which is due to the poor H_2 chemisorption on these metals compared to iron.

The FeO particles coated with carbon exhibit a bromate removal of 99%, probably due to H_2 chemisorption on metals and also through the carbon transfer electrons to Fe (III) to form Fe (II), and it donates electrons to bromate, resulting in its reduction, as represented in Scheme 1.

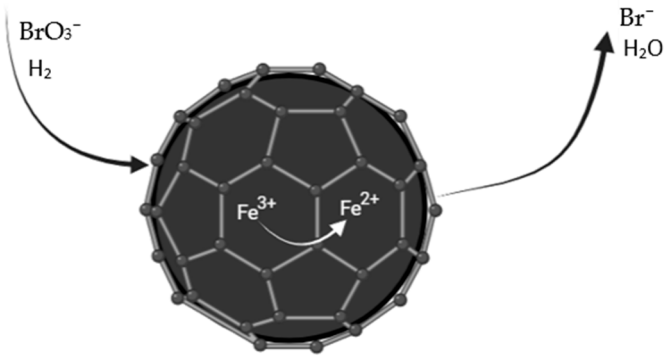

Scheme 1. Representative scheme of the metallic phase and its relationship with H_2 diffusion during chemisorption and the conversion reaction of BrO_3^- in a CFeO@CVD750 catalyst.

Perez-Coronado et al. [49] performed a test using only carbon nanotubes (CNTs) with H_2, observing a conversion similar to the non-catalytic run, showing that the presence of CNTs has no impact on this type of reaction. However, the presence of iron nanoparticles slightly increases bromate reduction, probably due to the transfer of electrons to CNTs.

As suggested in the literature, the mechanism involves the dissociative adsorption of hydrogen on the metal surface and the reaction between the adsorbed bromate ion and the hydrogen atoms [3]. Thus, the reaction mechanism proposed here involves the adsorption of bromate ions on the catalyst surface and their reduction via adsorbed and dissociated hydrogen. The bromide is consequently released into the bulk of the solution as the metal becomes oxidized.

2.2.3. Hydrogen-Free Experiment

To evaluate the influence of bromate adsorption, hydrogen was replaced with nitrogen, maintaining similar mixing conditions in the reactor. The results of these experiments are depicted in Figure 6.

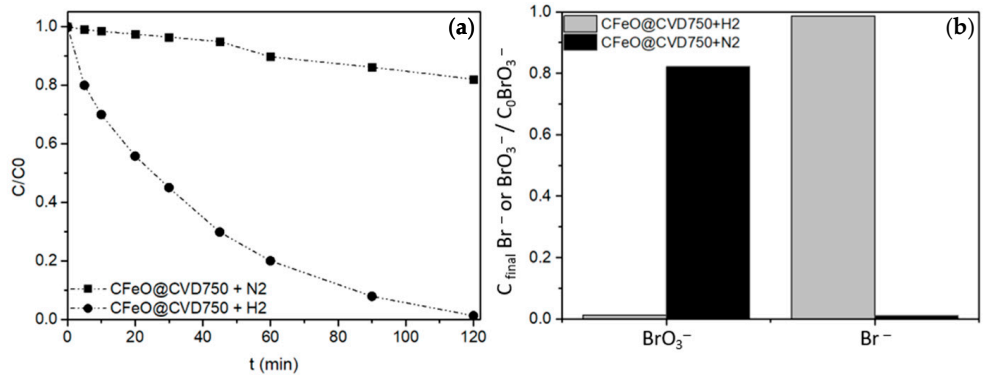

Figure 6. Dimensionless concentration of bromate during experiments using (**a**) CFeO@CVD750 with hydrogen and nitrogen and (**b**) bromate and bromide dimensionless concentrations after 120 min of reaction.

During bromate reduction with hydrogen, 99% removal was observed, while only 17% of bromate was removed from the solution in the absence of hydrogen, confirming that the activity associated with the material is related to its direct catalytic capacity in the hydrogenation of BrO_3^- to Br^-.

As suggested in the literature, the mechanism involves the dissociative adsorption of hydrogen on the metal surface and the reaction between the adsorbed bromate ion and hydrogen atoms [3,7,20].

2.2.4. Application to Real Water

The effectiveness of the catalysts in reducing bromate was tested using real water from a well. Details about the composition of this water are available in Table 3. Compared to ultrapure water, this well water sample presents a more complex matrix, which generally results in reduced catalyst performance [50]. Tests were carried out to evaluate the influence of organic and inorganic contents. As no bromate was found in the well water, a concentrated BrO_3^- solution, prepared from $NaBrO_3$, was added to the aqueous matrix to achieve a bromate concentration of 10 ppm. The CFeO@CVD750 catalyst was chosen due to the promising results obtained in the semi-batch system with ultrapure water (see Section 2.2.2), and Figure 7 shows the results of the catalytic reduction of bromate with hydrogen using both ultrapure water and the well water modified via the addition of bromate ion, as explained above.

Table 3. Characteristics of the water sample obtained from a well.

	Before Reaction	After Reaction
pH	7.17	7.25
Conductivity (μS cm^{-1})	238	237
TOC (mg L^{-1})	2.08	3.03
TC (mg L^{-1})	12.86	11.14
IC (mg L^{-1})	10.78	8.11
Br^- (mg L^{-1})	0.15	3.01
NO^{3-} (mg L^{-1})	0.65	0.33
NO^{2-} (mg L^{-1})	0.11	0.09
Cl^- (mg L^{-1})	0.38	0.01
SO_4^{2-} (mg L^{-1})	16.16	14.86
Na^+ (mg L^{-1})	12.28	11.54
NH_4^+ (mg L^{-1})	1.03	0.63
Ca^{2+} (mg L^{-1})	14.94	12.35
Mg^{2+} (mg L^{-1})	3.35	2.57

TOC—total organic carbon; TC—total carbon; IC—inorganic carbon.

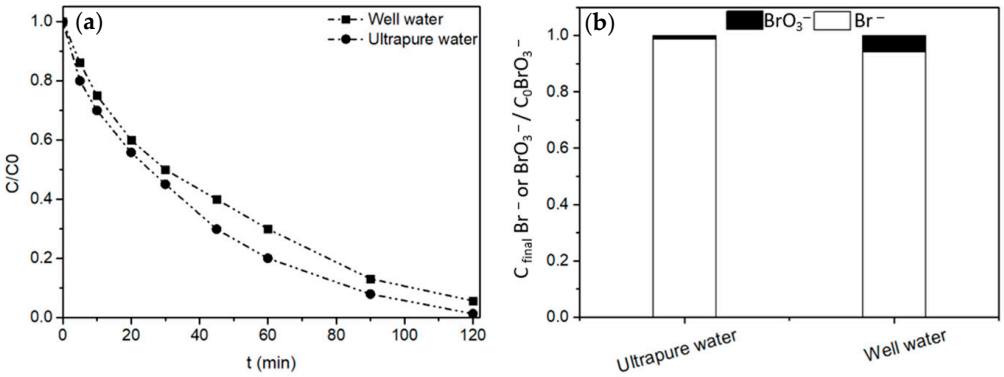

Figure 7. Dimensionless bromate concentration during hydrogen reduction over the catalyst CFeO@CVD750 using (**a**) different types of water and (**b**) bromate and bromide dimensionless concentrations after 120 min of reaction.

When analyzing Figure 7, it is possible to notice that the performance of the catalytic system slightly decreases from a conversion of 99% when using ultrapure water to 94% with the modified well water. This indicates that the presence of other ions and organic matter influences the catalytic activity. The mechanism of bromate reaction is revealed to be a process controlled via adsorption, and therefore, the presence of ions can trigger competition for adsorption on the active sites of the metal, inhibiting the reduction of bromate [4]. Chen et al. [20], when carrying out bromate reduction experiments in the presence of SO_4^{2-}, Cl^-, and Br^- ions to evaluate the impact of these anions, observed that the SO_4^{2-} ion, compared to Cl^- and Br^-, has a higher ionic charge. This results in stronger adsorption and, consequently, a more pronounced inhibition effect on bromate reduction. Furthermore, it was found that catalyst deactivation is more significant when the treated water is harder; that is, it contains higher levels of Ca^{2+} and Mg^{2+}. This leads to clogging of the catalyst due to salt deposition, making access to the catalyst difficult [51].

The textural properties of the CFeO@CVD750 catalyst were evaluated before and after the catalytic test, revealing that the specific surface area remained constant (S_{BET} = 63 m^2 g^{-1}). CFeO@CVD750 can be stable under the reaction conditions, preventing the formation of unwanted species that could reduce the surface area. The subsequent section describes catalyst reuse tests that were carried out to evaluate its continued activity.

2.2.5. Reutilization Experiments

The preparation and application of the magnetic particles coated with carbon were carried out to bring together the catalytic properties of the carbon materials and the magnetic character of the magnetic nanoparticles, making the catalyst easier to retain and recover by applying a magnetic field. In this view, the best material, CFeO @CVD750, was selected for reusing tests to investigate its stability and eventual deactivation. After a typical first experiment, the catalyst was dried and used again under the same experimental conditions to assess its activity. This procedure was repeated four times, as shown in Figure 8, revealing that the catalyst exhibited the same performance in the four consecutive runs.

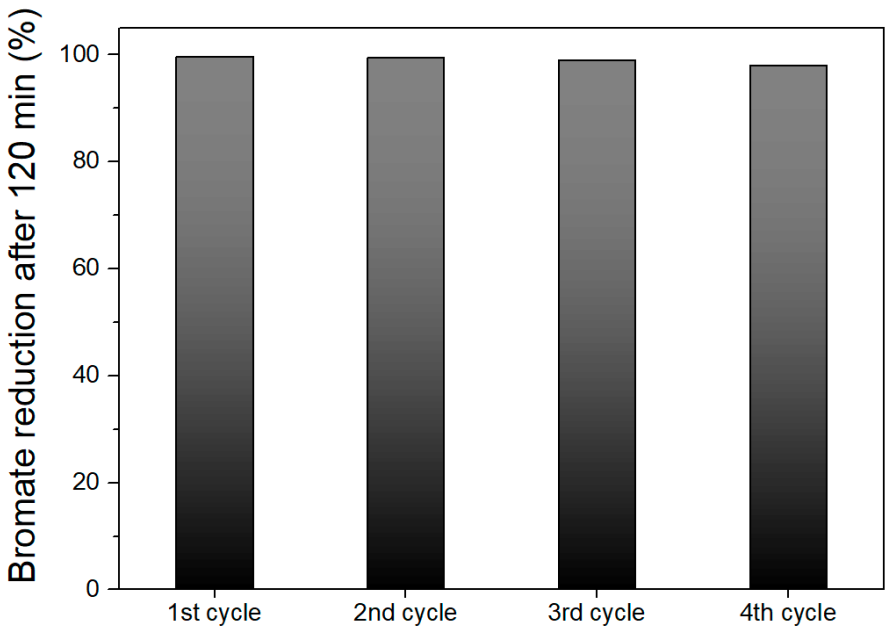

Figure 8. Reuse of the CFeO@CVD750 catalyst in the removal of bromate.

Therefore, we may conclude that the CFeO@CVD750 catalyst is stable for the removal of bromate.

3. Materials and Methods

3.1. Preparation of Materials

The magnetic nanoparticles (MNPs) of FeO, MnFeO, CoFeO, and CuFeO were prepared using the co-precipitation method [26]. First, 40 mmol of $FeCl_3.6H_2O$ and 20 mmol of $FeCl_2.4H_2O$ were dissolved in 50 mL of 2M HCl solution. Then, 500 mL of a 1.5 M NaOH solution was added to this solution, with vigorous mechanical stirring, at room temperature. A black precipitate immediately formed, and stirring continued for 2 h.

MnFeO, CoFeO, and CuFeO nanoparticles were synthesized through a precipitation process. To prepare MnFeO, CoFeO, or CuFeO, we dissolved 40 mmol of $FeCl_3{\cdot}6H_2O$ in 80 mL of distilled water and 20 mmol of $MnSO_4{\cdot}H_2O$, $Co(NO_3)_2{\cdot}6H_2O$, or $Cu(NO_3)_2{\cdot}3H_2O$ in 10 mL of HCl 0.5 M. Both solutions were heated to 50 °C, mixed, and then quickly added to 400 mL of a 100 °C 3 M NaOH solution while being vigorously mechanically stirred. The black precipitate formed immediately in all three cases, and stirring continued for 2 h at 100 °C. After this period, the reaction mixtures were cooled to room temperature, followed by magnetic separation of the precipitates, which were subjected to repeated washing with distilled water.

After the synthesis, the MNPs were coated with carbon via the chemical vapor deposition process (CVD) using ethane as a carbon source [26]. Briefly, the MNPs were thermally treated under a N_2 flow up to 400 °C, and then, the reduction step was carried out in an H_2 atmosphere for 2 h. After that, the temperature was increased up to 750 °C to coat the magnetic nanoparticles with carbon using ethane as carbon precursor (samples CFeO@CVD750, CMnFeO@CVD750, CCoFeO@CVD750, and CCuFeO@CVD750). Then, the coated MNPs were cooled under N_2 until achieving room temperature.

For comparison purposes, an iron catalyst supported on commercial multi-walled carbon nanotubes (Nanocyl 3100, from Nanocyl, Sambreville, Belgium) was also obtained and tested (sample 2%Fe_CNT). This material was prepared using the incipient impregnation method. After impregnation, the sample was dried at 100 °C for 24 h, heat-treated under a N_2 flow at 400 °C for 1 h, and reduced under a H_2 flow for 3 h [26].

3.2. Characterization of Materials

The textural and chemical properties of the materials were characterized by N_2 adsorption at −196 °C, thermogravimetric analysis (TG), temperature-programmed reduction (TPR), transmission electron microscopy (TEM), and X-ray diffraction (XRD). Further details can be found elsewhere [26,37]. The scanning electron microscopy coupled with energy-dispersive X-ray spectroscopy (SEM-EDS) was performed using the high-resolution environmental scanning electron microscope (Schottky), with X-ray microanalysis and the analysis of diffused electron diffraction patterns: Quanta 400FEG ESEM/EDAX Genesis X4M (FEI Company, Hillsboro, OR, USA).

3.3. Catalytic Tests

The catalytic reduction of bromate in water (10 mg L^{-1}) was carried out in a semi-batch reactor in the presence of hydrogen at ambient temperature and atmospheric pressure. Initially, 395 mL of ultrapure water and 200 mg of catalyst were placed in the reactor at a constant stirring speed of 700 rpm. The reactor was fed with a stream of H_2 for 15 min to ensure no air in the solution (H_2 flow rate = 50 cm^3 min^{-1}). After that, 5 mL of concentrated bromate solution, prepared from $NaBrO_3$, was added to the reactor. Small samples were taken from the reactor to determine bromate and bromide ions at different reaction times. The solution pH was measured throughout the experiments, and it remained practically constant (around 6). Each catalyst was tested at least two times, and the measured conversions demonstrated remarkable reproducibility, with a maximum variation of 2% from the average. The concentrations of bromate and bromide were analyzed via ion chromatography (Metrohm 881 Compact IC Pro, Herisau, Switzerland) using an appropriate anion column (Metrosep A Supp 7 250/4 from Metrohm) with a 3.6 Mm Na_2CO_3 stationary phase. The determination of the amount of total organic carbon in the

well water sample was carried out using the TOC-L equipment (Shimadzu TOC-5000A, Tokyo, Japan).

4. Conclusions

The use of magnetic nanoparticles (MNPs) was successfully demonstrated for the reduction of bromate in water for the first time. The CVD coating procedure proved to be a simple and accessible technique to synthesize efficient catalysts. This procedure allowed for taking advantage of the catalytic properties of the metal–carbon materials and the efficient recovery attained due to their magnetic nature.

FeO particles allow a 76% reduction of bromate into bromide after 120 min of reaction, whereas the introduction of Co, Mn, or Cu in the FeO particles decreases the activity. Coating the MNPs with carbon improves the catalytic activity, with the highest bromate reduction being achieved with the CFeO@CVD750 catalyst. Due to its magnetic nature, this catalyst was easily recovered at the end of the first cycle and applied in three more cycles without losing its catalytic properties, which is very attractive in terms of practical applications.

Supplementary Materials: The following supporting information can be downloaded at: https://www.mdpi.com/article/10.3390/catal14020149/s1, Figure S1: TPR profiles of (a) CoFeO and (b) MnFeO before and after carbon coating with CVD; Figure S2: XRD patterns of FeO (a) and CFeO@CVD750 materials (b). The black line represents the Rietveld refinement, and the green line shows the difference between the experimental data and the fit obtained via the Rietveld refinement.

Author Contributions: P.S.F.R.: methodology, investigation, and writing—original draft. O.S.G.P.S.: supervision, conceptualization, methodology, and writing—review and editing. J.J.M.Ó.: conceptualization and writing—review and editing. M.F.R.P.: supervision, conceptualization, funding acquisition, and writing—review and editing. All authors have read and agreed to the published version of the manuscript.

Funding: This work was supported by national funds through FCT/MCTES (PIDDAC): LSRE-LCM, UIDB/50020/2020 (https://doi.org/10.54499/UIDP/50020/2020) and UIDP/50020/2020 (https://doi.org/10.54499/UIDP/50020/2020); and ALiCE, LA/P/0045/2020 (https://doi.org/10.54499/LA/P/0045/2020). O.S.G.P.S. acknowledges FCT funding under the Scientific Employment Stimulus—Institutional Call, CEECINST/00049/2018 (https://doi.org/10.54499/CEECINST/00049/2018/CP1524/CT0008).

Data Availability Statement: Data are available on request from the corresponding author.

Conflicts of Interest: The authors declare no conflict of interest.

References

1. Xu, J.-H.; Gao, N.-Y.; Zhao, D.-Y.; Zhang, W.-X.; Xu, Q.-K.; Xiao, A.-H. Efficient reduction of bromate in water by nano-iron hydroxide impregnated granular activated carbon (Fe-GAC). *Chem. Eng. J.* **2015**, *275*, 189–197. [CrossRef]
2. Krasner, S.W.; Glaze, W.H.; Weinberg, H.S.; Daniel, P.A.; Najm, I.N. Formation and Control of Bromate During Ozonation of Waters Containing Bromide. *J. AWWA* **1993**, *85*, 73–81. [CrossRef]
3. Restivo, J.; Soares, O.S.G.P.; Órfão, J.J.M.; Pereira, M.F.R. Metal assessment for the catalytic reduction of bromate in water under hydrogen. *Chem. Eng. J.* **2015**, *263*, 119–126. [CrossRef]
4. Costa, J.M.C.B.D.; Barbosa, J.R.M.; Restivo, J.; Orge, C.A.; Nogueira, A.; Castro-Silva, S.; Pereira, M.F.R.; Soares, O.S.G.P. Engineering of Nanostructured Carbon Catalyst Supports for the Continuous Reduction of Bromate in Drinking Water. *C* **2022**, *8*, 21. [CrossRef]
5. Freitas, C.M.A.S.; Soares, O.S.G.P.; Órfão, J.J.M.; Fonseca, A.M.; Pereira, M.F.R.; Neves, I.C. Highly efficient reduction of bromate to bromide over mono and bimetallic ZSM5 catalysts. *Green Chem.* **2015**, *17*, 4247–4254. [CrossRef]
6. Shen, W.; Lin, F.; Jiang, X.; Li, H.; Ai, Z.; Zhang, L. Efficient removal of bromate with core-shell Fe@Fe_2O_3 nanowires. *Chem. Eng. J.* **2017**, *308*, 880–888. [CrossRef]
7. Soares, O.S.G.P.; Ramalho, P.S.F.; Fernandes, A.; Órfão, J.J.M.; Pereira, M.F.R. Catalytic bromate reduction in water: Influence of carbon support. *J. Environ. Chem. Eng.* **2019**, *7*, 103015. [CrossRef]
8. World Health Organization. *Bromide in Drinking-Water: Background Document for Development of WHO Guidelines for Drinking-Water Quality*; World Health Organization: Geneva, Switzerland, 2009.

9. Wiśniewski, J.A.; Kabsch-Korbutowicz, M.; Łakomska, S. Removal of bromate ions from water in the processes with ion-exchange membranes. *Sep. Purif. Technol.* **2015**, *145*, 75–82. [CrossRef]
10. Wiśniewski, J.A.; Kabsch-Korbutowicz, M. Bromate removal in the ion-exchange process. *Desalination* **2010**, *261*, 197–201. [CrossRef]
11. Huang, X.; Wang, L.; Zhou, J.; Gao, N. Photocatalytic decomposition of bromate ion by the UV/P25-Graphene processes. *Water Res.* **2014**, *57*, 1–7. [CrossRef]
12. Zhao, X.; You, Y.; Huang, S.; Cheng, F.; Chen, P.; Li, H.; Zhang, Y. Facile construction of reduced graphene oxide supported three-dimensional polyaniline/WO2.72 nanobelt-flower as a full solar spectrum light response catalyst for efficient photocatalytic conversion of bromate. *Chemosphere* **2019**, *222*, 781–788. [CrossRef] [PubMed]
13. Huang, W.-J.; Cheng, Y.-L. Effect of characteristics of activated carbon on removal of bromate. *Sep. Purif. Technol.* **2008**, *59*, 101–107. [CrossRef]
14. Ji, H.; Wu, W.; Li, F.; Yu, X.; Fu, J.; Jia, L. Enhanced adsorption of bromate from aqueous solutions on ordered mesoporous Mg-Al layered double hydroxides (LDHs). *J. Hazard. Mater.* **2017**, *334*, 212–222. [CrossRef] [PubMed]
15. Kishimoto, N.; Matsuda, N. Bromate Ion Removal by Electrochemical Reduction Using an Activated Carbon Felt Electrode. *Environ. Sci. Technol.* **2009**, *43*, 2054–2059. [CrossRef] [PubMed]
16. Yao, F.; Yang, Q.; Sun, J.; Chen, F.; Zhong, Y.; Yin, H.; He, L.; Tao, Z.; Pi, Z.; Wang, D.; et al. Electrochemical reduction of bromate using noble metal-free nanoscale zero-valent iron immobilized activated carbon fiber electrode. *Chem. Eng. J.* **2019**, 123588. [CrossRef]
17. Peldszus, S.; Andrews, S.A.; Souza, R.; Smith, F.; Douglas, I.; Bolton, J.; Huck, P.M. Effect of medium-pressure UV irradiation on bromate concentrations in drinking water, a pilot-scale study. *Water Res.* **2004**, *38*, 211–217. [CrossRef] [PubMed]
18. Bensalah, N.; Liu, X.; Abdel-Wahab, A. Bromate reduction by ultraviolet light irradiation using medium pressure lamp. *Int. J. Environ. Stud.* **2013**, *70*, 566–582. [CrossRef]
19. Nurlan, N.; Akmanova, A.; Lee, W. The Use of H2 in Catalytic Bromate Reduction by Nanoscale Heterogeneous Catalysts. *Nanomaterials* **2022**, *12*, 1212. [CrossRef]
20. Chen, H.; Xu, Z.; Wan, H.; Zheng, J.; Yin, D.; Zheng, S. Aqueous bromate reduction by catalytic hydrogenation over Pd/Al_2O_3 catalysts. *Appl. Catal. B* **2010**, *96*, 307–313. [CrossRef]
21. Zhang, Z.; Luo, Y.; Guo, Y.; Shi, W.; Wang, W.; Zhang, B.; Zhang, R.; Bao, X.; Wu, S.; Cui, F. Pd and Pt nanoparticles supported on the mesoporous silica molecular sieve SBA-15 with enhanced activity and stability in catalytic bromate reduction. *Chem. Eng. J.* **2018**, *344*, 114–123. [CrossRef]
22. Chen, X.; Huo, X.; Liu, J.; Wang, Y.; Werth, C.J.; Strathmann, T.J. Exploring beyond palladium: Catalytic reduction of aqueous oxyanion pollutants with alternative platinum group metals and new mechanistic implications. *Chem. Eng. J.* **2017**, *313*, 745–752. [CrossRef]
23. Franch, C.; Rodríguez-Castellón, E.; Reyes-Carmona, Á.; Palomares, A.E. Characterization of (Sn and Cu)/Pd catalysts for the nitrate reduction in natural water. *Appl Catal A-Gen* **2012**, *425–426*, 145–152. [CrossRef]
24. Barrabés, N.; Just, J.; Dafinov, A.; Medina, F.; Fierro, J.L.G.; Sueiras, J.E.; Salagre, P.; Cesteros, Y. Catalytic reduction of nitrate on Pt-Cu and Pd-Cu on active carbon using continuous reactor: The effect of copper nanoparticles. *Appl. Catal. B Environ.* **2006**, *62*, 77–85. [CrossRef]
25. Pereira, C.; Pereira, A.; Carlos, F.; Mariana, R.; Ricardo, M.; Garcia, M.; Guedes, M.; Pedro, B.T.; Jean Marc, G.; Araújo, J.; et al. Superparamagnetic MFe_2O_4 (M = Fe, Co, Mn) Nanoparticles: Tuning the Particle Size and Magnetic Properties through a Novel One-Step Coprecipitation Route. *Chem. Mater.* **2012**, *24*, 1496–1504. [CrossRef]
26. Pereira, L.; Dias, P.; Soares, O.S.G.P.; Ramalho, P.S.F.; Pereira, M.F.R.; Alves, M.M. Synthesis, characterization and application of magnetic carbon materials as electron shuttles for the biological and chemical reduction of the azo dye Acid Orange 10. *Appl. Catal. B* **2017**, *212*, 175–184. [CrossRef]
27. Xie, J.; Liu, G.; Eden, H.S.; Ai, H.; Chen, X. Surface-Engineered Magnetic Nanoparticle Platforms for Cancer Imaging and Therapy. *Acc. Chem. Res.* **2011**, *44*, 883–892. [CrossRef] [PubMed]
28. Chen, X.; Gambhir, S.S.; Cheon, J. Theranostic Nanomedicine. *Acc. Chem. Res.* **2011**, *44*, 841. [CrossRef] [PubMed]
29. Suber, L.; Marchegiani, G.; Olivetti, E.S.; Celegato, F.; Coïsson, M.; Tiberto, P.; Allia, P.; Barrera, G.; Pilloni, L.; Barba, L.; et al. Pure magnetic hard fct FePt nanoparticles: Chemical synthesis, structural and magnetic properties correlations. *Mater. Chem. Phys.* **2014**, *144*, 186–193. [CrossRef]
30. Long, Y.; Xie, M.; Niu, J.; Wang, P.; Ma, J. Preparation of acid–base bifunctional core–shell structured $Fe_3O_4@SiO_2$ nanoparticles and their cooperative catalytic activity. *Appl. Surf. Sci.* **2013**, *277*, 288–292. [CrossRef]
31. Xu, X.; Wu, H.; Li, Z.; Sun, X.; Wang, Z. Iron oxide-silver magnetic nanoparticles as simple heterogeneous catalysts for the direct inter/intramolecular nucleophilic substitution of π-activated alcohols with electron-deficient amines. *Tetrahedron* **2015**, *71*, 5254–5259. [CrossRef]
32. Shokouhimehr, M. Magnetically Separable and Sustainable Nanostructured Catalysts for Heterogeneous Reduction of Nitroaromatics. *Catalysts* **2015**, *5*, 534–560. [CrossRef]
33. Heidari, F.; Hekmati, M.; Veisi, H. Magnetically separable and recyclable $Fe_3O_4@SiO_2$/isoniazide/Pd nanocatalyst for highly efficient synthesis of biaryls by Suzuki coupling reactions. *J. Colloid Interface Sci.* **2017**, *501*, 175–184. [CrossRef]

34. Hu, J.; Chen, G.; Lo, I.M.C. Selective Removal of Heavy Metals from Industrial Wastewater Using Maghemite Nanoparticle: Performance and Mechanisms. *J. Environ. Eng.* **2006**, *132*, 709–715. [CrossRef]
35. Ali, Q.; Ahmed, W.; Lal, S.; Sen, T. Novel Multifunctional Carbon Nanotube Containing Silver and Iron Oxide Nanoparticles for Antimicrobial Applications in Water Treatment. *Mater. Today Proc.* **2017**, *4*, 57–64. [CrossRef]
36. Funari, V.; Mantovani, L.; Vigliotti, L.; Tribaudino, M.; Dinelli, E.; Braga, R. Superparamagnetic iron oxides nanoparticles from municipal solid waste incinerators. *Sci. Total Environ.* **2018**, *621*, 687–696. [CrossRef] [PubMed]
37. Orge, C.; Soares, O.; Ramalho, P.; Pereira, M.; Faria, J. Magnetic Nanoparticles for Photocatalytic Ozonation of Organic Pollutants. *Catalysts* **2019**, *9*, 703. [CrossRef]
38. Li, M.; Zhou, X.; Sun, J.; Fu, H.; Qu, X.; Xu, Z.; Zheng, S. Highly effective bromate reduction by liquid phase catalytic hydrogenation over Pd catalysts supported on core-shell structured magnetites: Impact of shell properties. *Sci. Total Environ.* **2019**, *663*, 673–685. [CrossRef] [PubMed]
39. Li, Q.; Jiang, S.; Ji, S.; Shi, D.; Yan, J.; Huo, Y.; Zhang, Q. Magnetically Recyclable Cu-BTC@SiO2@Fe3O4 Catalysts and Their Catalytic Performance for the Pechmann Reaction. *Ind. Eng. Chem. Res.* **2014**, *53*, 14948–14955. [CrossRef]
40. Chen, H.; Zhang, P.; Tan, W.; Jiang, F.; Tang, R. Palladium supported on amino functionalized magnetic MCM-41 for catalytic hydrogenation of aqueous bromate. *RSC Adv.* **2014**, *4*, 38743–38749. [CrossRef]
41. Lin, K.-Y.A.; Chen, S.-Y. Catalytic Reduction of Bromate Using ZIF-Derived Nanoscale Cobalt/Carbon Cages in the Presence of Sodium Borohydride. *ACS Sustain. Chem. Eng.* **2015**, *3*, 3096–3103. [CrossRef]
42. Kameoka, S.; Tanabe, T.; Tsai, A.P. Spinel CuFe2O4: A precursor for copper catalyst with high thermal stability and activity. *Catal. Lett.* **2005**, *100*, 89–93. [CrossRef]
43. Pinto, M.; Ramalho, P.S.F.; Moreira, N.F.F.; Gonçalves, A.G.; Nunes, O.C.; Pereira, M.F.R.; Soares, O.S.G.P. Application of magnetic nanoparticles for water purification. *Environ. Adv.* **2020**, *2*, 100010. [CrossRef]
44. Yang, Q.; Choi, H.; Al-Abed, S.R.; Dionysiou, D.D. Iron–cobalt mixed oxide nanocatalysts: Heterogeneous peroxymonosulfate activation, cobalt leaching, and ferromagnetic properties for environmental applications. *Appl. Catal. B* **2009**, *88*, 462–469. [CrossRef]
45. Zhang, L.; Wu, Y. Sol-Gel Synthesized Magnetic $MnFe_2O_4$ Spinel Ferrite Nanoparticles as Novel Catalyst for Oxidative Degradation of Methyl Orange. *J. Nanomater.* **2013**, *2013*, 640940. [CrossRef]
46. Hagen, J. Heterogeneous Catalysis: Fundamentals. In *Industrial Catalysis: A Practical Approach*; John Wiley & Sons: Hoboken, NJ, USA, 2015; pp. 99–217.
47. Xie, L.; Shang, C.; Zhou, Q. Effect of Fe(III) on the bromate reduction by humic substances in aqueous solution. *J. Environ. Sci.* **2008**, *20*, 257–261. [CrossRef] [PubMed]
48. Zhong, Y.; Yang, Q.; Luo, K.; Wu, X.; Li, X.; Liu, Y.; Tang, W.; Zeng, G.; Peng, B. Fe(II)–Al(III) layered double hydroxides prepared by ultrasound-assisted co-precipitation method for the reduction of bromate. *J. Hazard. Mater.* **2013**, *250–251*, 345–353. [CrossRef]
49. Perez-Coronado, A.M.; Soares, O.S.G.P.; Calvo, L.; Rodriguez, J.J.; Gilarranz, M.A.; Pereira, M.F.R. Catalytic reduction of bromate over catalysts based on Pd nanoparticles synthesized via water-in-oil microemulsion. *Appl. Catal. B* **2018**, *237*, 206–213. [CrossRef]
50. Soares, O.S.G.P.; Órfão, J.J.M.; Gallegos-Suarez, E.; Castillejos, E.; Rodríguez-Ramos, I.; Pereira, M.F.R. Nitrate reduction over a Pd-Cu/MWCNT catalyst: Application to a polluted groundwater. *Environ. Technol.* **2012**, *33*, 2353–2358. [CrossRef]
51. Cerrillo, J.L.; Palomares, A.E. A Review on the Catalytic Hydrogenation of Bromate in Water Phase. *Catalysts* **2021**, *11*, 365. [CrossRef]